星・惑星系の形成過程 入門

中本泰史 (東工大)

1. 形成過程の概観
2. 分子雲の重力収縮
3. 原始惑星系円盤
4. 固体微粒子の進化
5. 微惑星から惑星へ
6. 惑星系の形成

微惑星から惑星へ

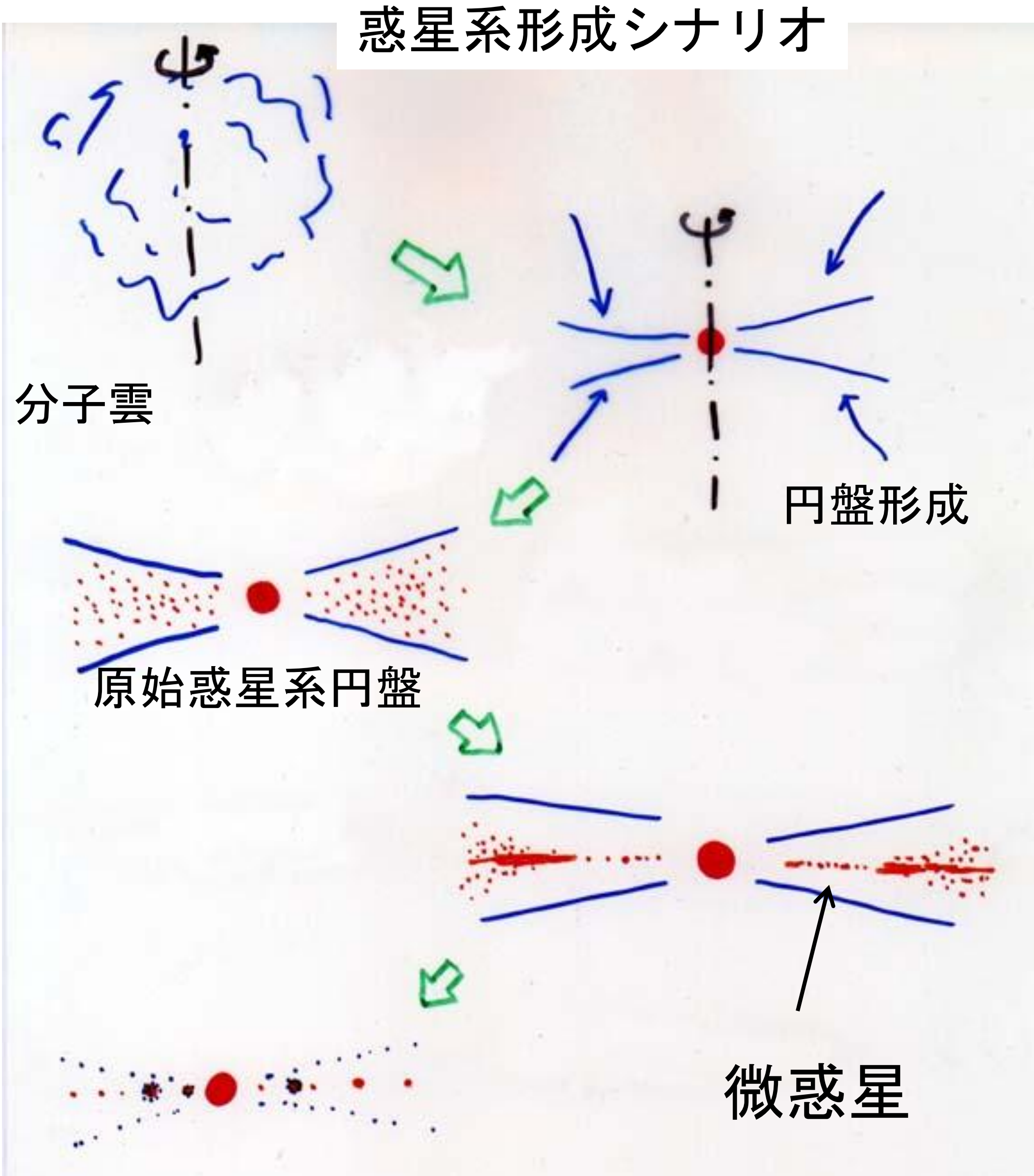
惑星系形成シナリオ
分子雲
円盤形成
原始惑星系円盤
微惑星

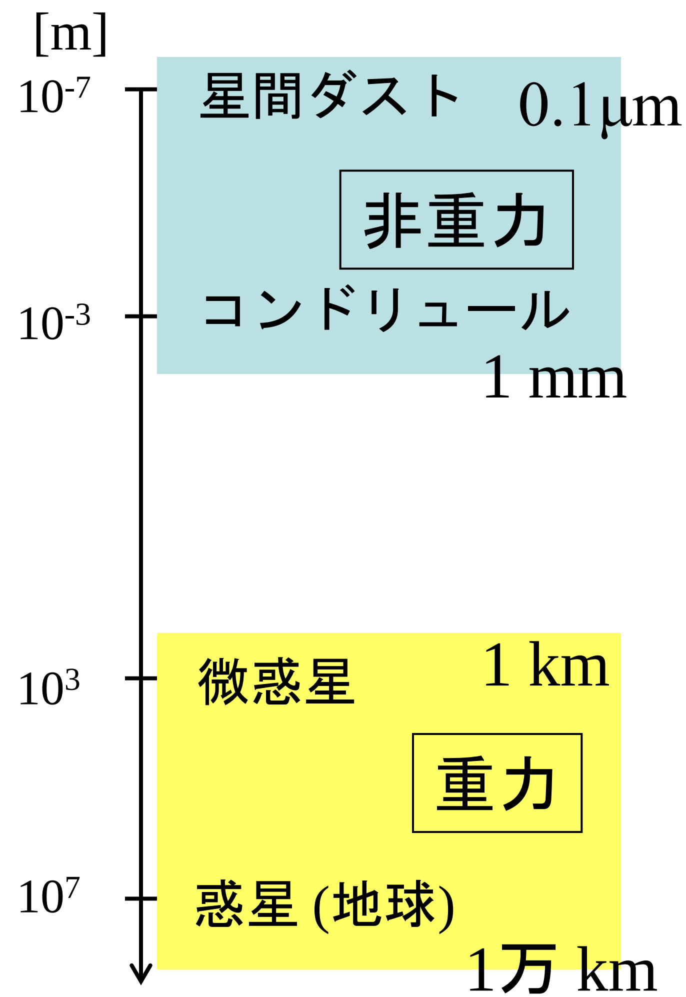
[m]
10^{-7}
10^{-3}
10^{3}
10^{7}
星間ダスト
0.1μm
非重力
コンドリュール
1 mm
微惑星
1 km
重力
惑星 (地球)
1万 km

微惑星の合体成長

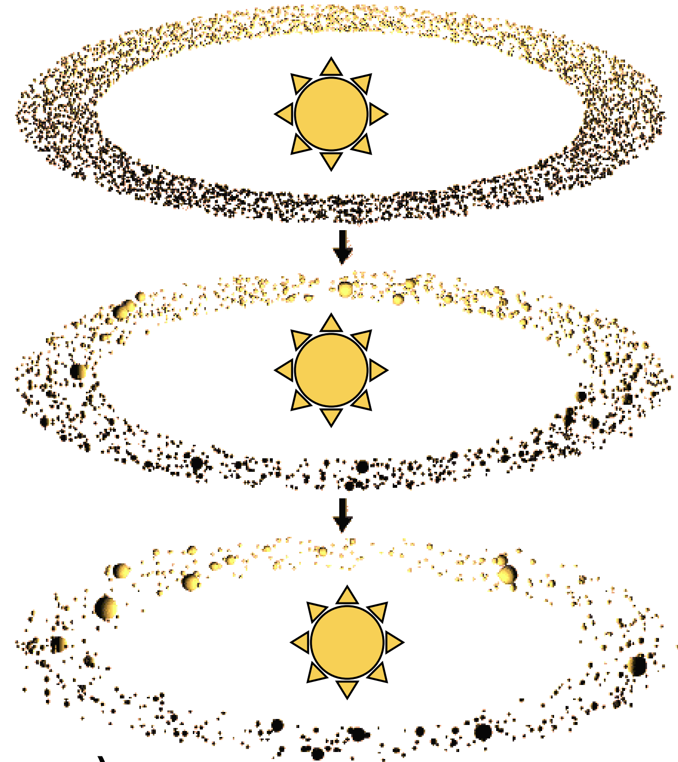

井田・小久保

・太陽の周りを回る天体群
・多体相互作用

N体計算：運動を調べる

$$m_i \frac{d^2\mathbf{r}_i}{dt^2} = -\frac{GMm_i}{\left|\mathbf{r}_i - \mathbf{r}_{\mathrm{sun}}\right|^3}\left(\mathbf{r}_i - \mathbf{r}_{\mathrm{sun}}\right) - \sum_j \frac{Gm_i m_j}{\left|\mathbf{r}_i - \mathbf{r}_j\right|^3}\left(\mathbf{r}_i - \mathbf{r}_j\right)$$

衝突したら合体

*N*体計算の例

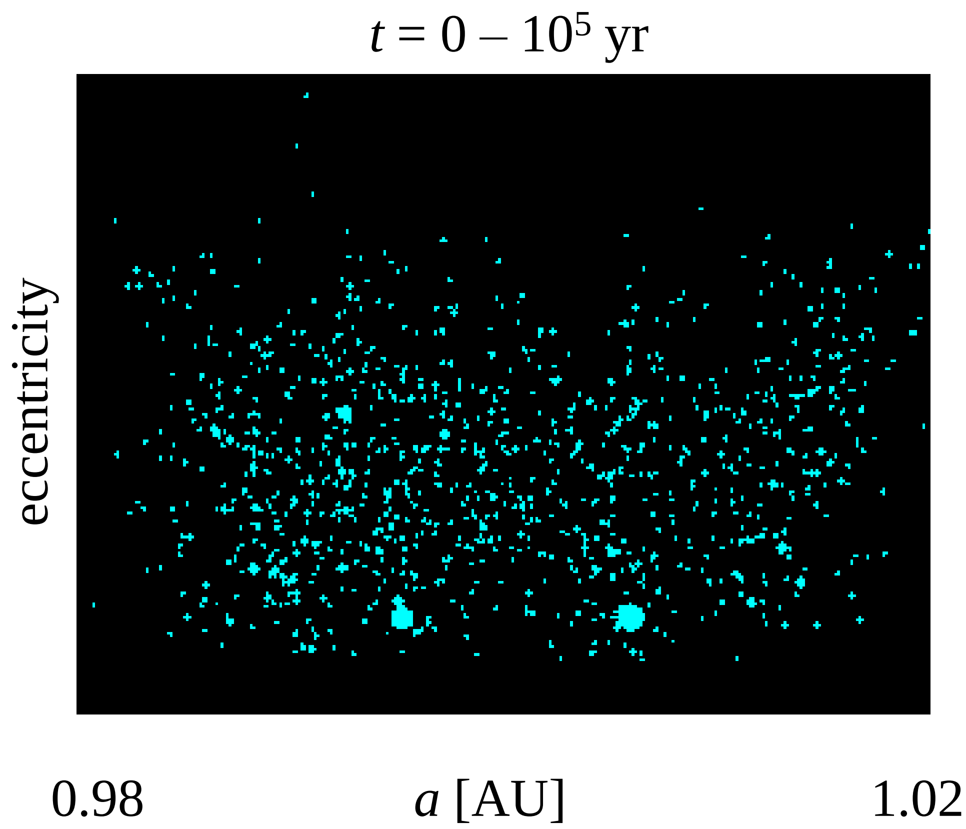

Kokubo & Ida 1996

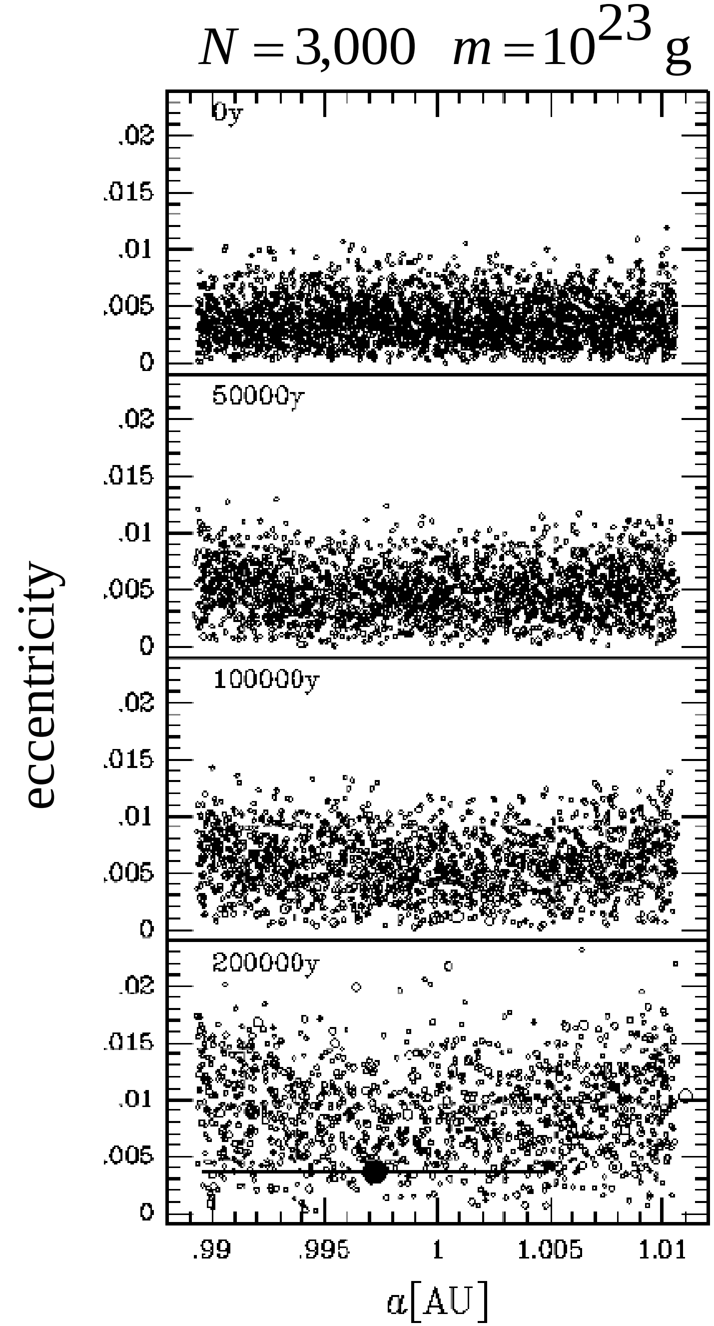

Kokubo & Ida 2000

暴走成長

・大きな質量の天体が
先に成長

・質量大 → e 小

エネルギー等分配

Particle-in-a-Box近似で
よく理解できる

自由空間(外場なしの空間)内
での運動・相互作用として近似

$N = 3{,}000 \quad m = 10^{23}\,\mathrm{g}$

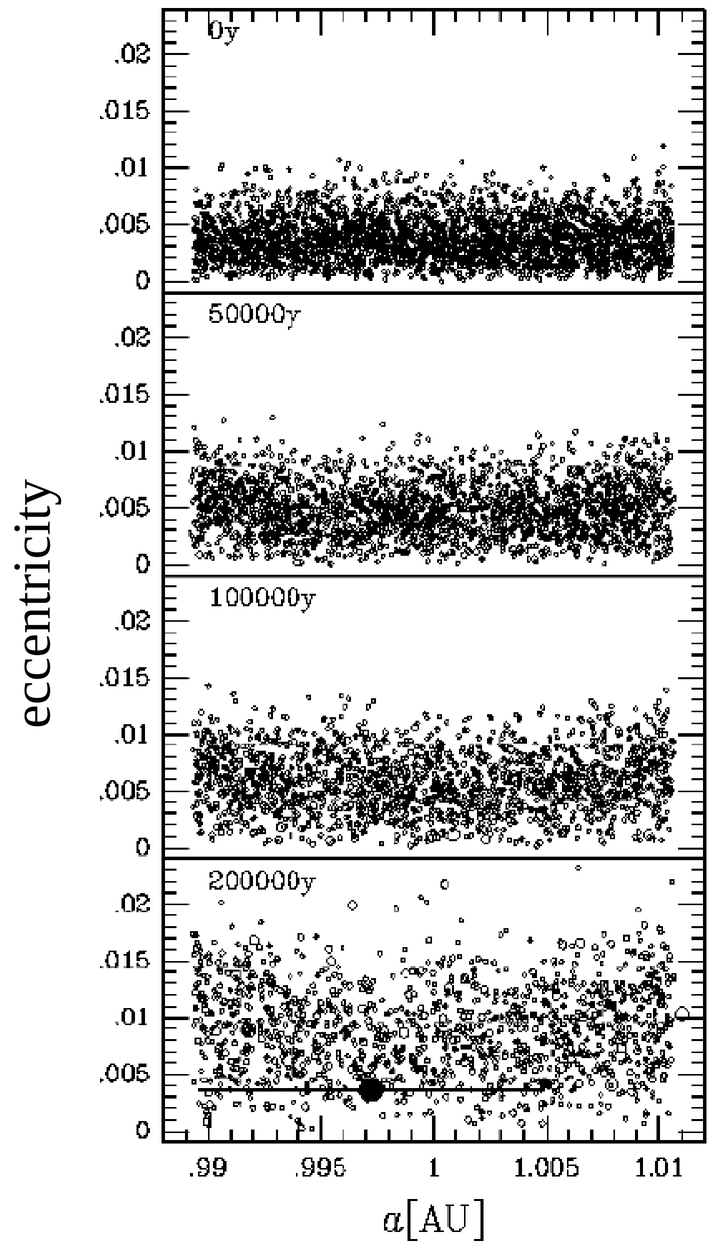

Kokubo & Ida 2000

Particle-in-a-box近似

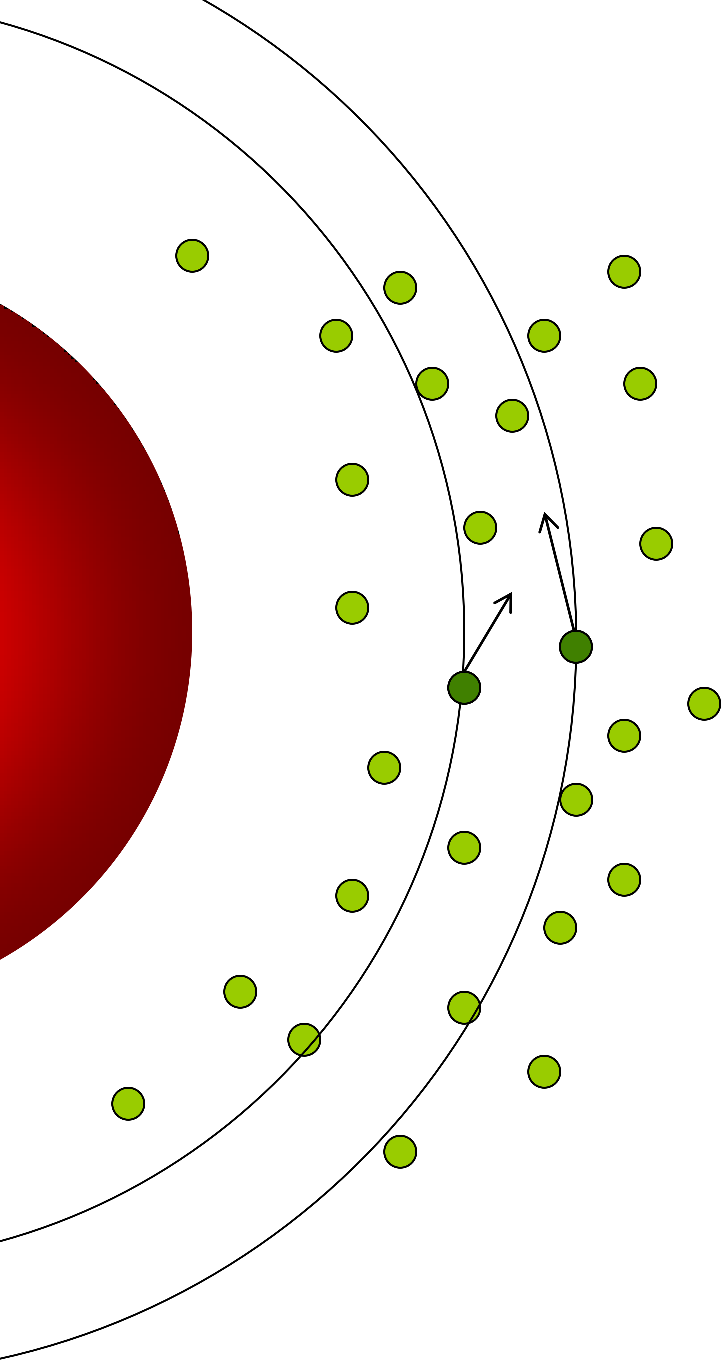

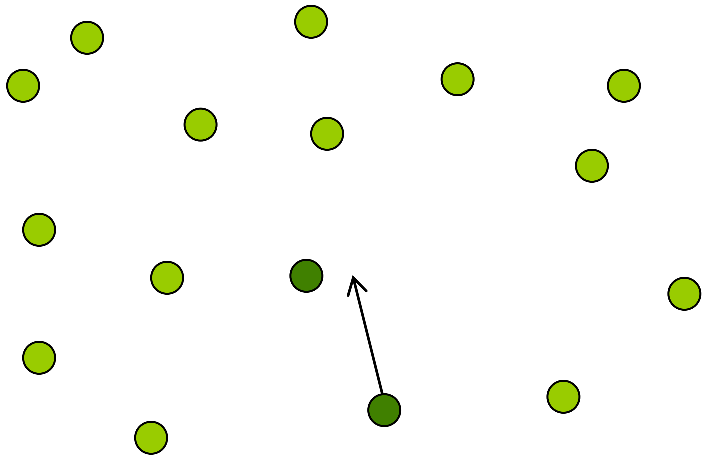

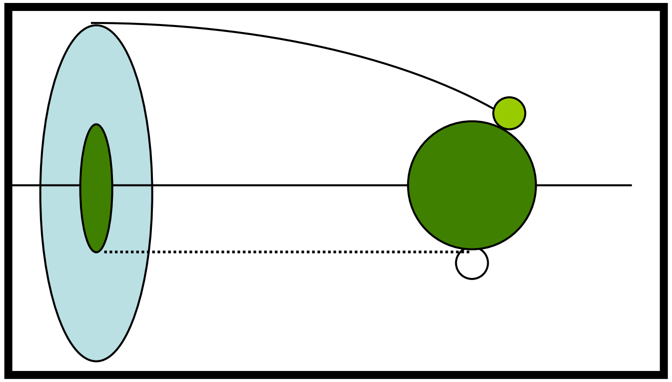

楕円運動の場合

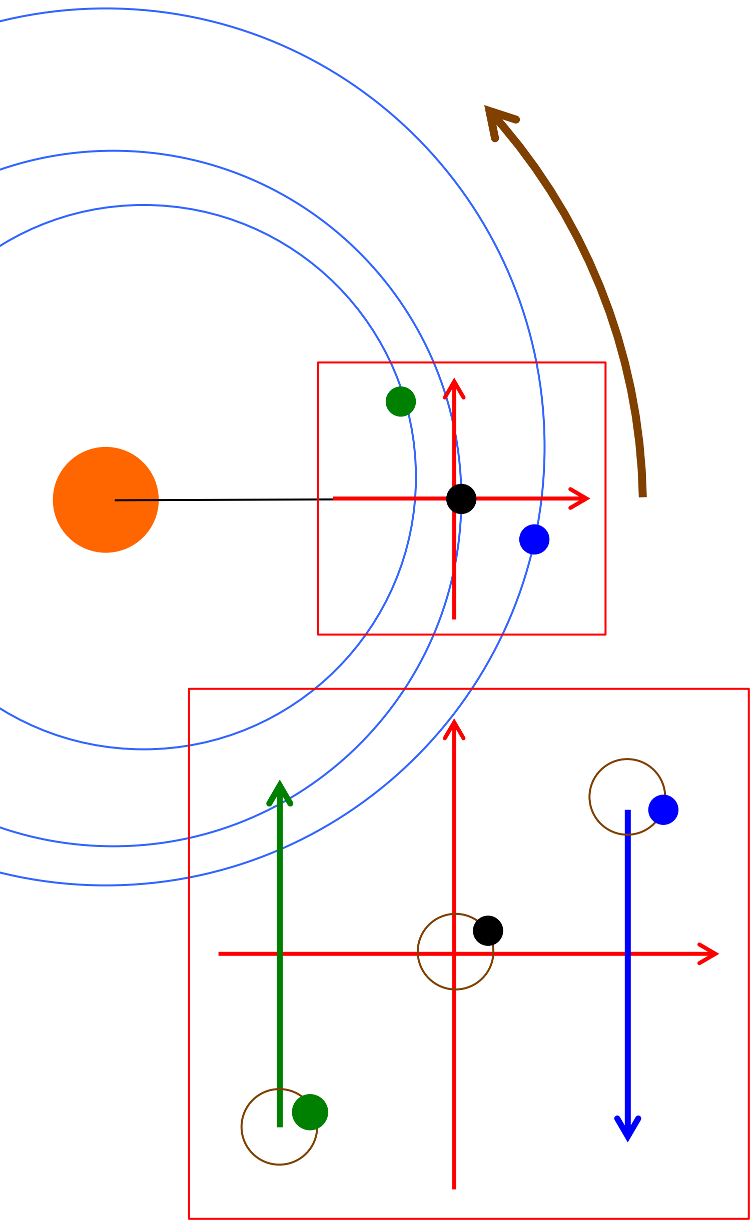

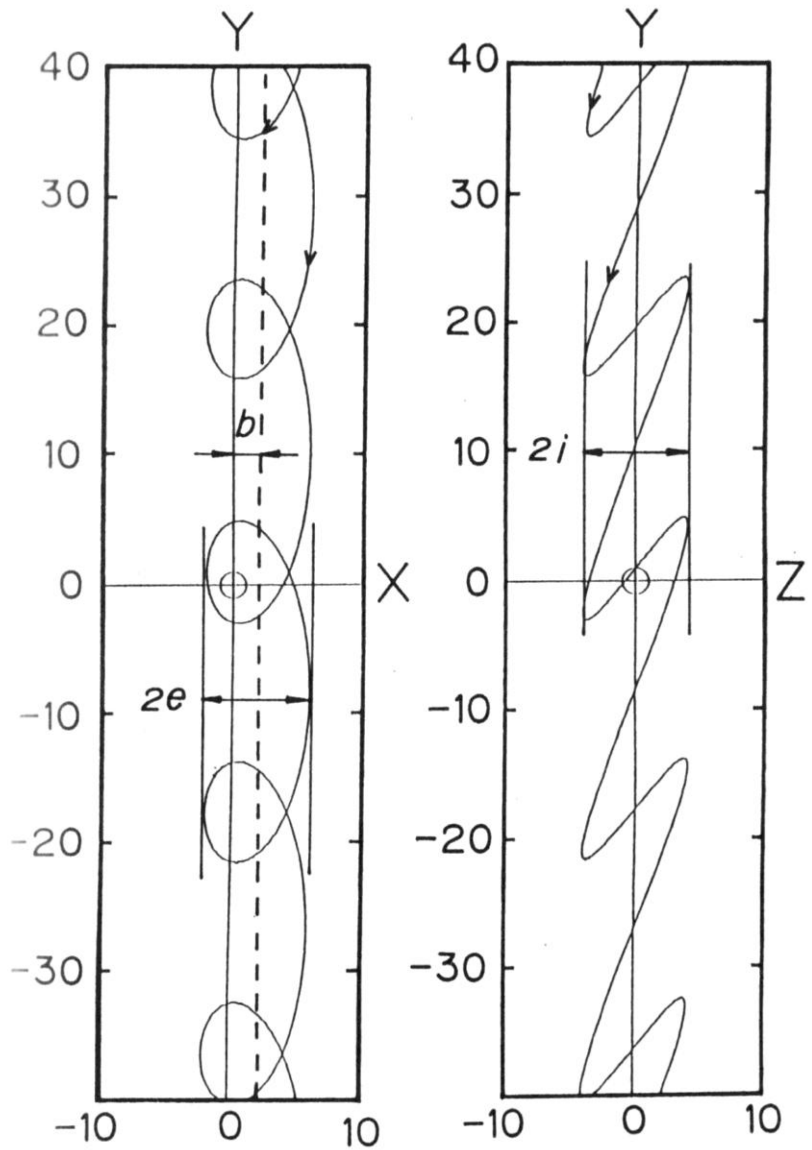

Fig. 2. A typical example of an unperturb

Hasegawa et al. 1988

of relative motion projected onto the x-y plane (left) and y-z plane (right). The circle at the origin denotes the Hill sphere. The dashed

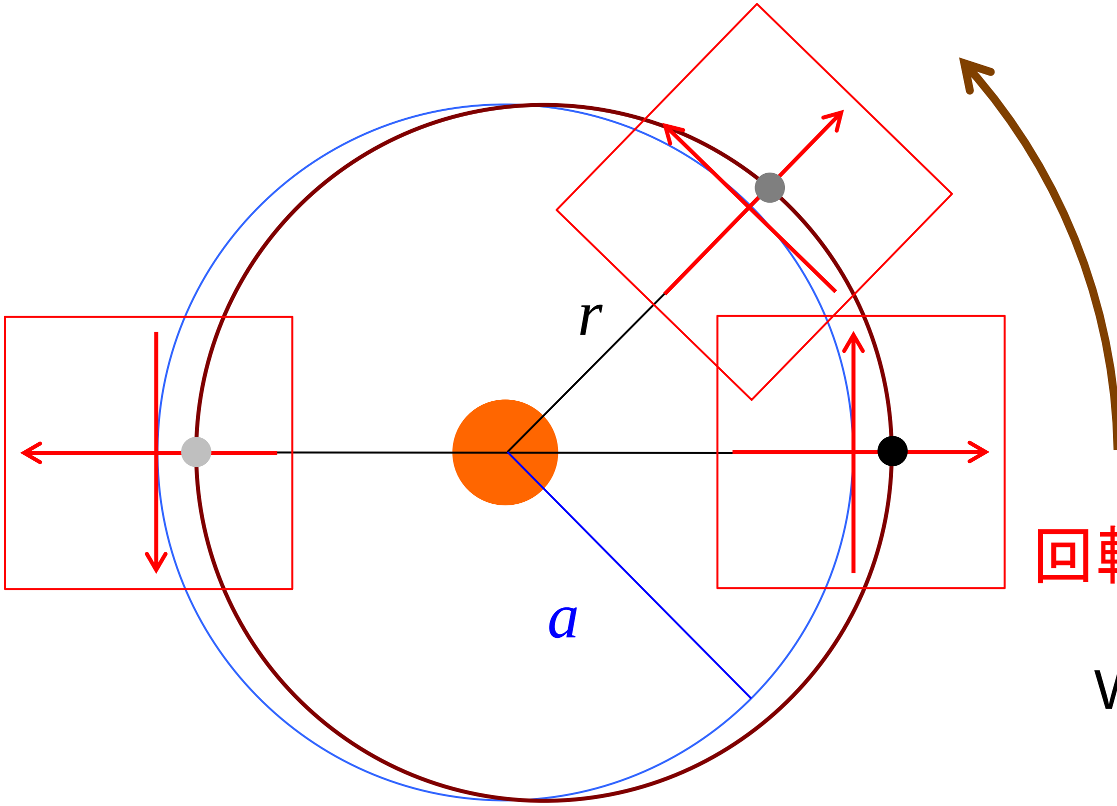

回転座標系

$$\Omega_K = \sqrt{\frac{GM}{a^3}}$$

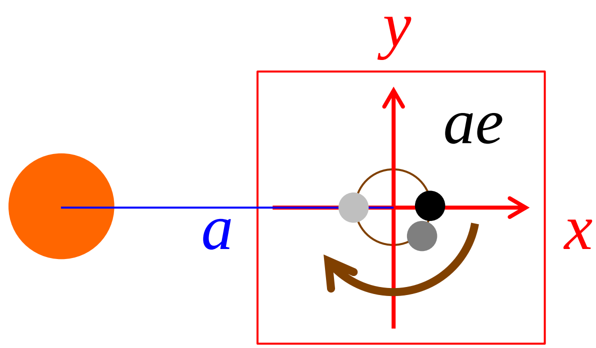

エピサイクル運動
(周転円運動)
周期：T_K

$$v = ae\Omega_K = V_K e$$

重力相互作用する 2体の運動

Nishida 1983

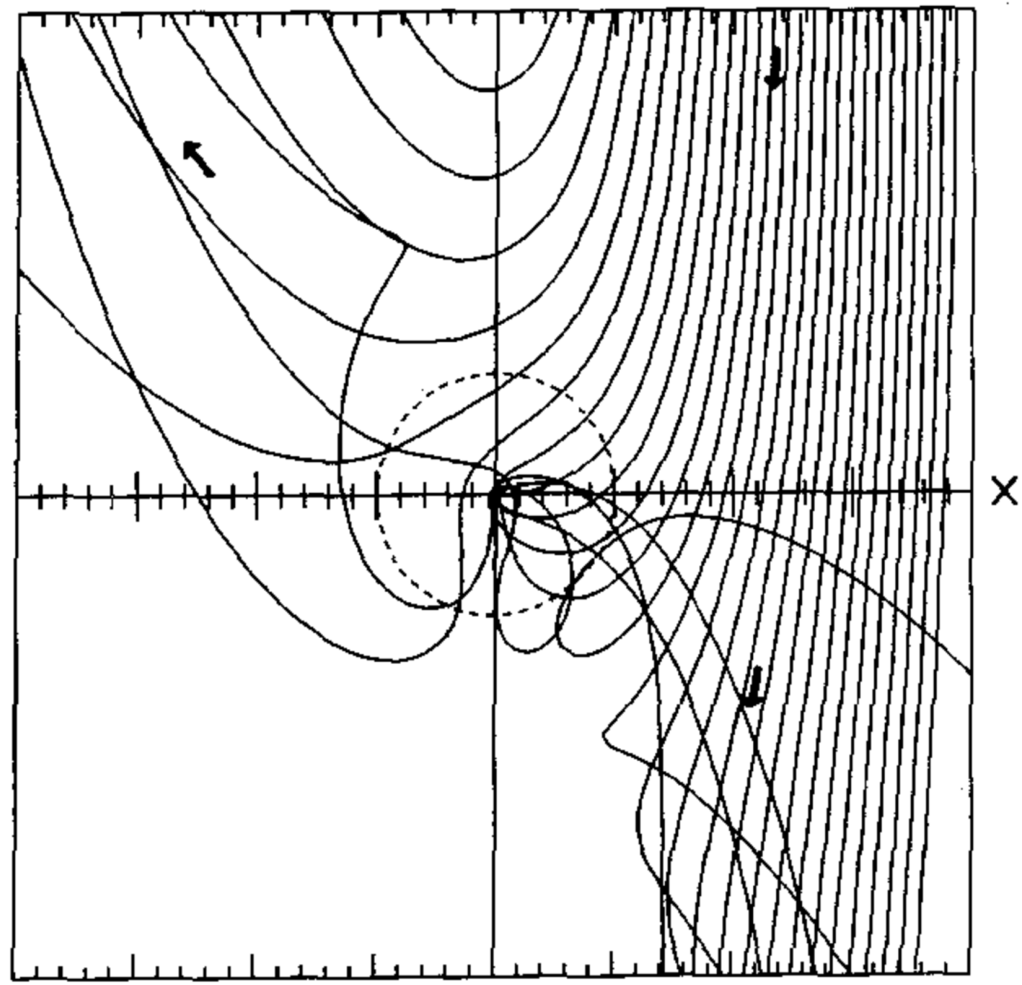

Fig. 2. Examples of particle orbits with various values of $\tilde{b}_i$ and with $\tilde{e}_i \simeq 0$. The dotted circle represents the Hill sphere. All the particles with $1.75 < \tilde{b}_i < 2.50$ enter the sphere.

微惑星同士の衝突・合体・成長

$$\frac{dm_0}{dt} = m_1 n \sigma v = m_1 n \cdot \pi R^2 \left(1 + \frac{2G(m_0 + m_1)}{R v^2}\right) \cdot v$$

$$R = R_0 + R_1$$

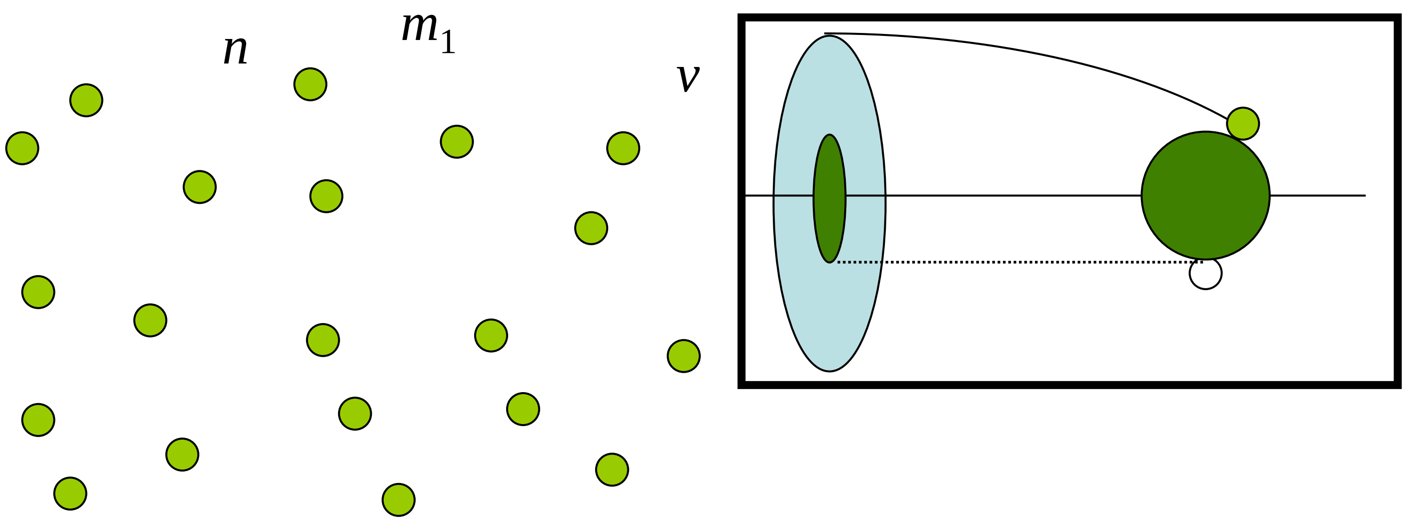

微惑星同士の衝突・合体・成長

$$\frac{dm_0}{dt} = m_1 n \sigma v = m_1 n \cdot \pi R^2 \left(1 + \frac{2G(m_0 + m_1)}{R v^2}\right) \cdot v$$

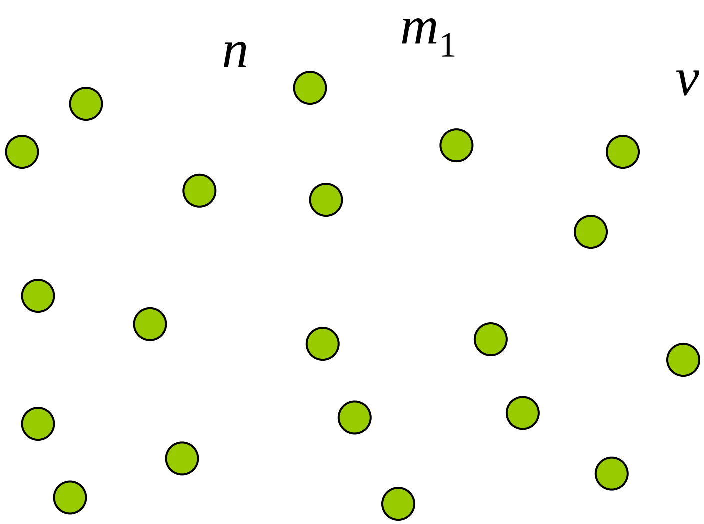

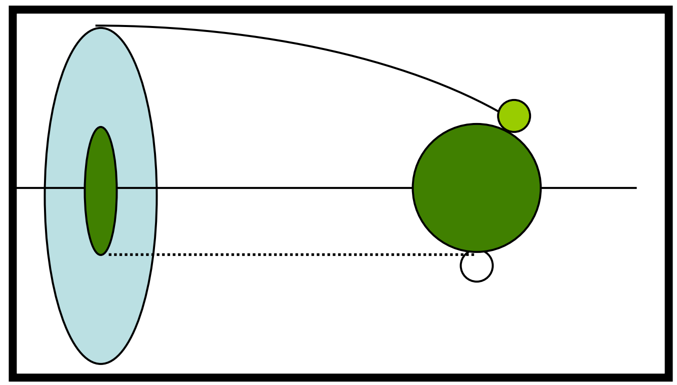

$$\frac{dm_0}{dt} \sim m_1 n \cdot \pi R^2 \frac{2G(m_0 + m_1)}{R v^2} \cdot v \sim m_1 n \cdot \pi R_0 \frac{2G m_0}{v} \propto m_0^{4/3}$$

$$\frac{dm_0}{dt} \propto m_0^{4/3}$$ のとき

初期 $m_0 > m_1$

$$\frac{d}{dt}\left(\frac{m_0}{m_1}\right) = \frac{m_0}{m_1}\left(\frac{1}{m_0}\frac{dm_0}{dt} - \frac{1}{m_1}\frac{dm_1}{dt}\right) \propto \frac{m_0}{m_1}\left(m_0^{1/3} - m_1^{1/3}\right) > 0$$

質量差が広がる！　→　暴走成長

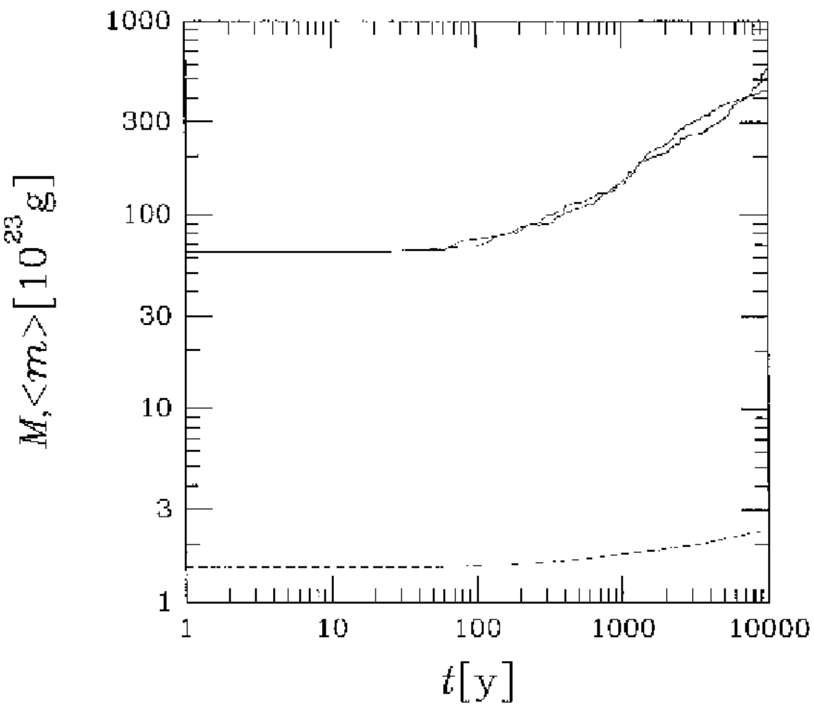

2個の大天体

小天体集団の平均値

FIG. 2 Time evolution of the masses of the two protoplanets (solid curves) and the mean mass of the planetesimals (dashed curve).

Kokubo & Ida 1998

エネルギー等分配

- 自由空間中の粒子集団（気体分子運動論）
- 平衡状態

$$\frac{1}{2}m_1 v_1^2 \approx \frac{1}{2}m_2 v_2^2$$

$m_1 > m_2$　ならば

$$v_1 < v_2$$

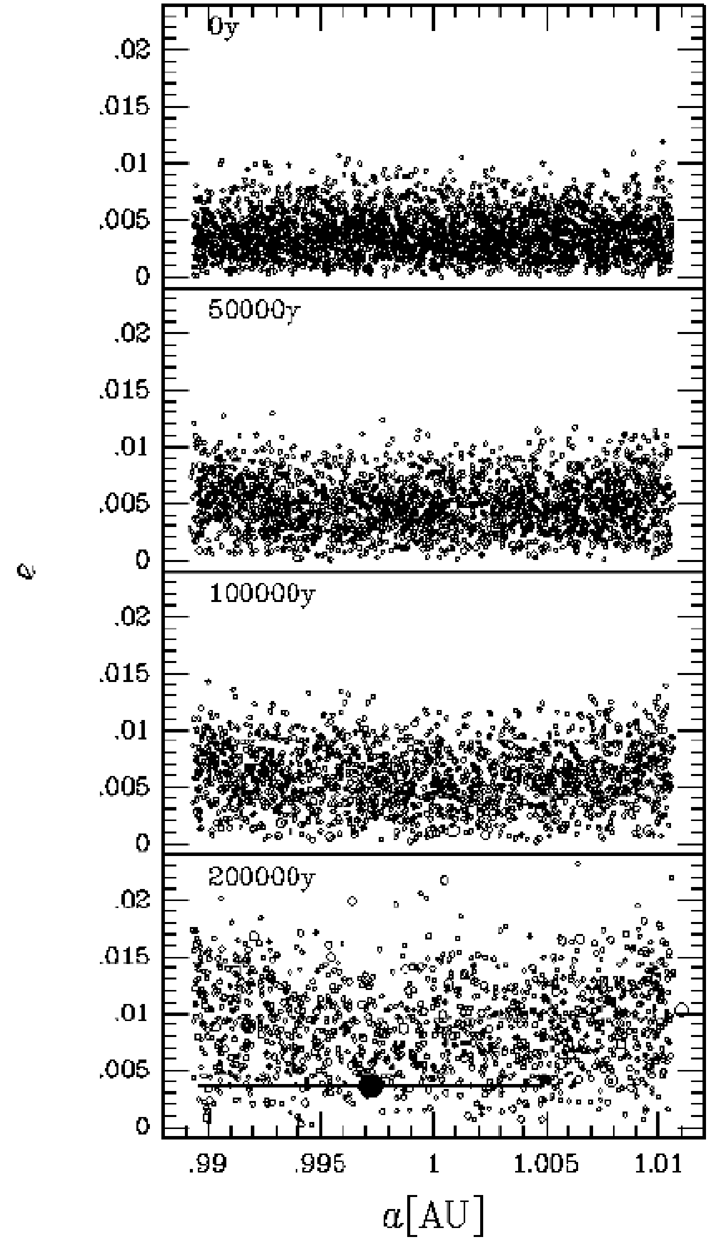

Kokubo & Ida 2000

寡占的成長

- 大天体の重力のため，小天体の e が増大
- 軌道反発

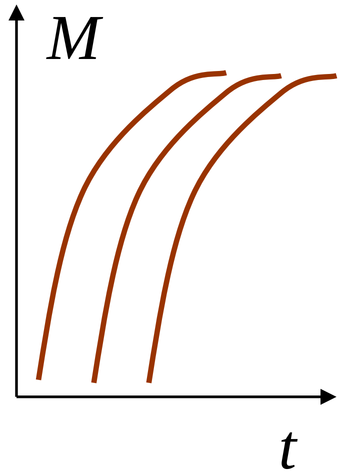

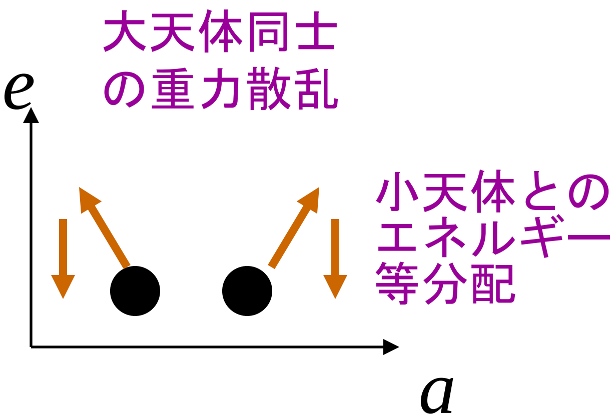

$$\Delta a \approx 10\text{-}15\, r_{\mathrm{H}}$$

$$r_{\mathrm{H}} = \left(\frac{M}{3M_{\mathrm{sun}}} \right)^{1/3} a$$

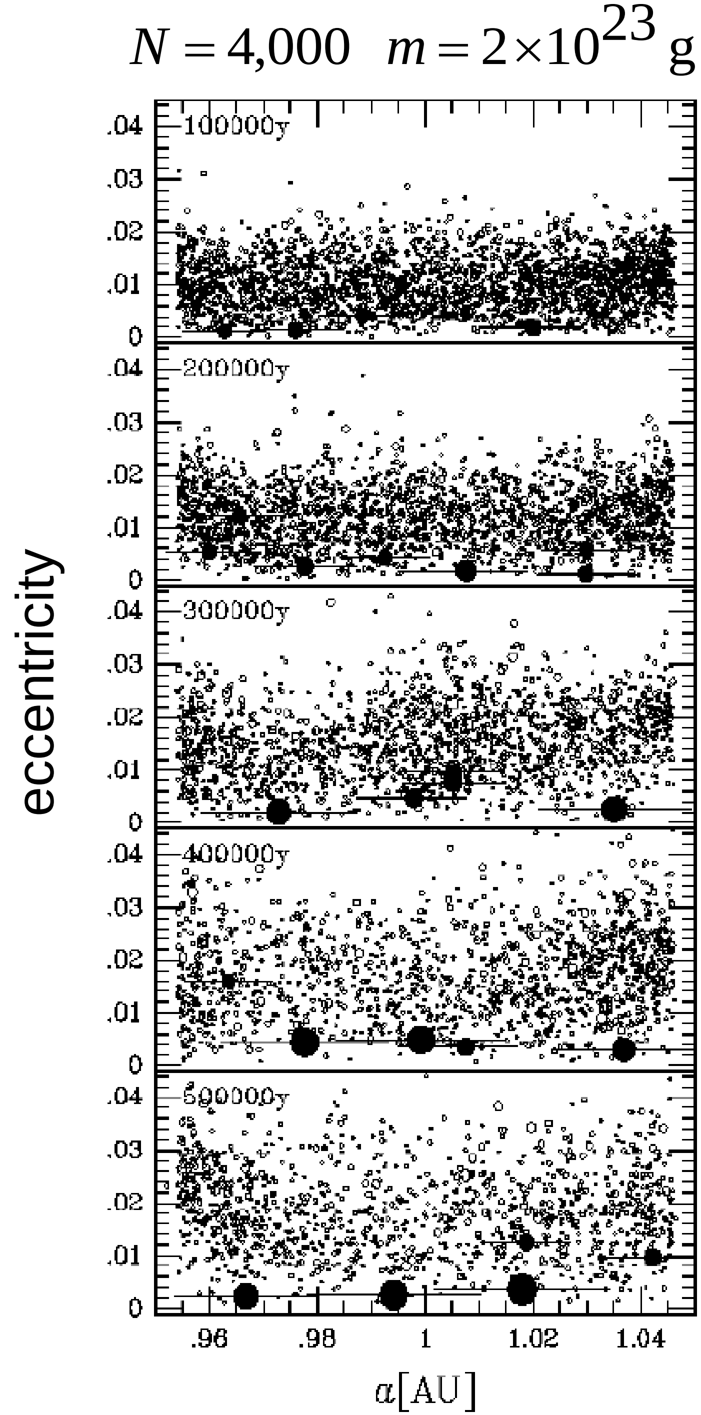

孤立質量

$\Delta r \sim 10 r_H$

＋円盤モデル
(初期微惑星空間分布)

→ 原始惑星の質量

$$M_{iso} = 2\pi r \times 10 r_H \times \Sigma_{solid}$$

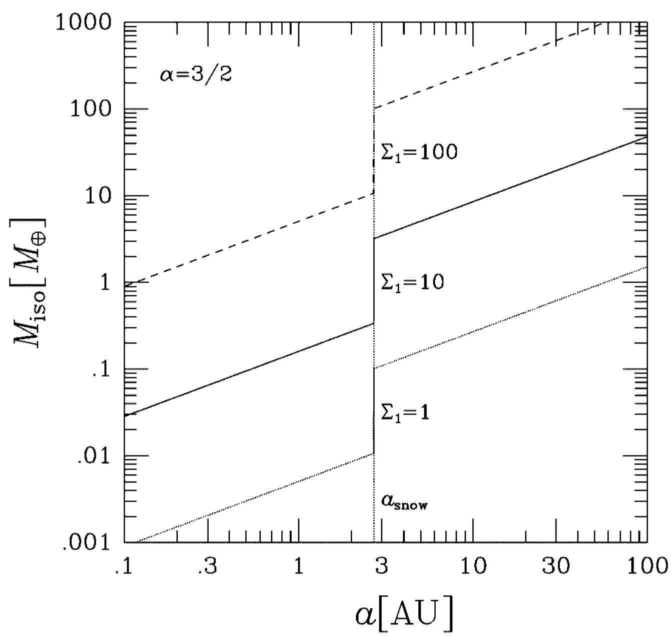

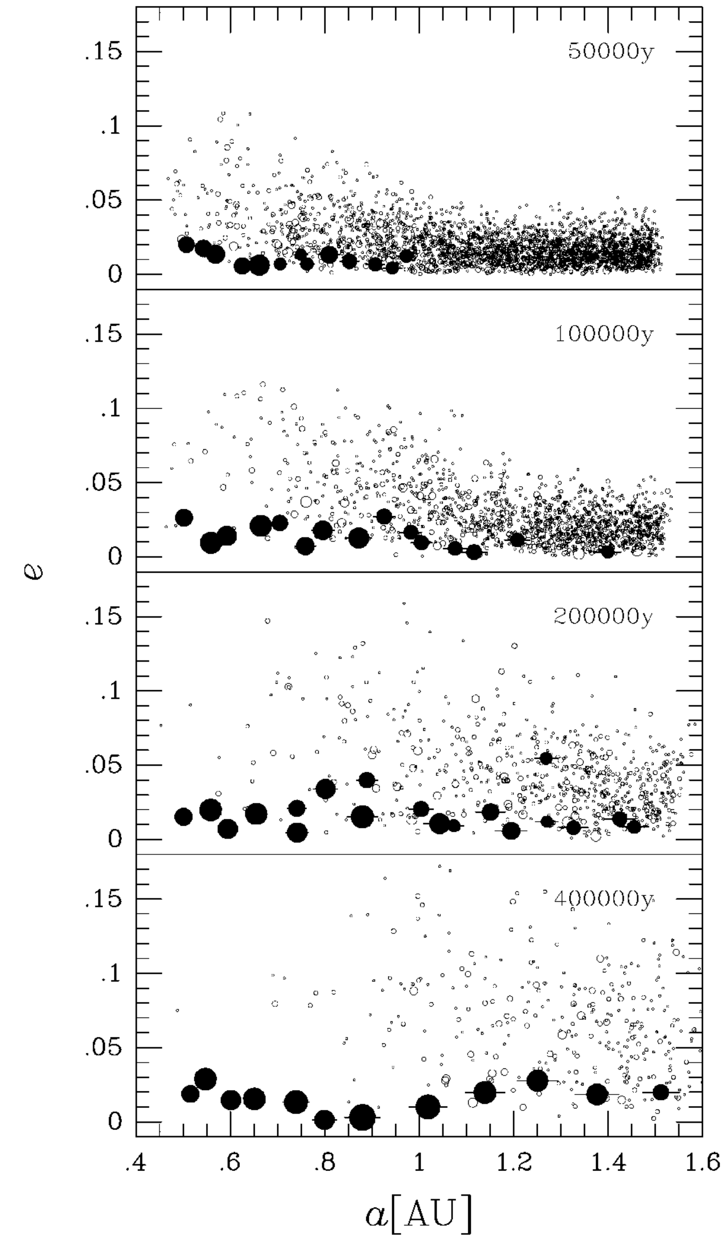

Kokubo & Ida 2002

FIG. 1*a*

$\rightarrow$ 巨大衝突時代

e 上昇

問題：

- 太陽系惑星は e 小 $\leftarrow$ 説明可能？
- 火星質量が小さいのはなぜ？
- …

Hansen 2009

初期質量分布

$0.7\mathrm{AU} < a < 1\ \mathrm{AU}$

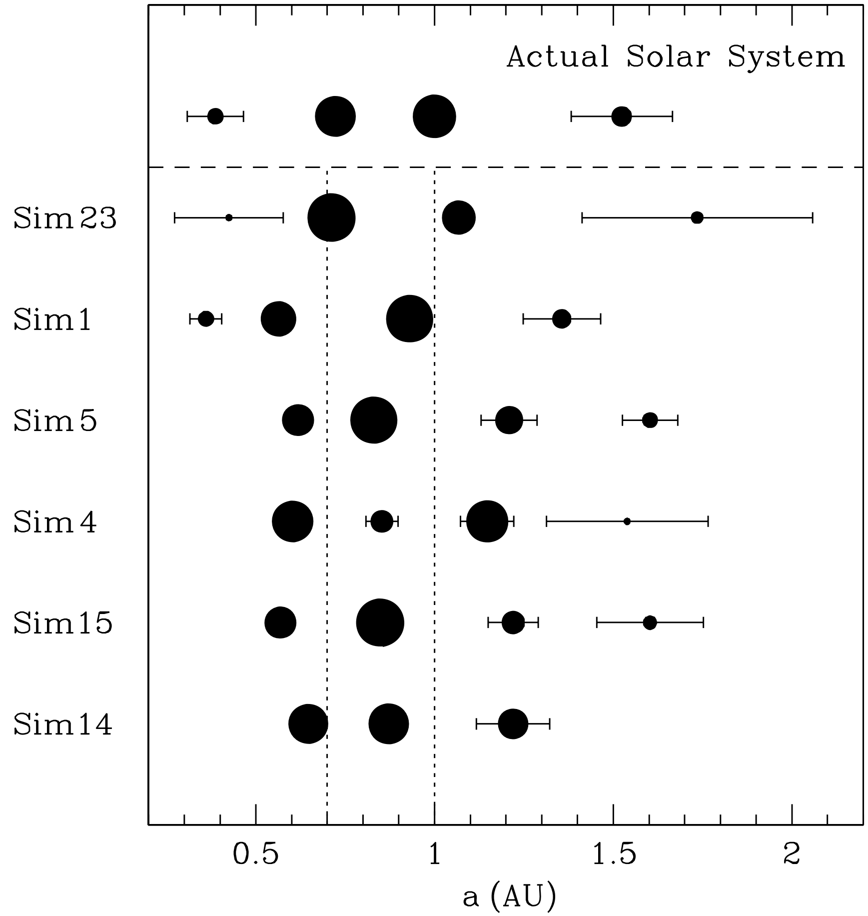

Figure 2. Top system is the observed terrestrial planets, Mercury, Venus, Earth and Mars. Below that are six realizations of a simulation which begins with 2 Earth masses of material spread uniformly between 0.7 and 1 AU (as indicated by the vertical dotted lines). The size of the plotted points scales as the cube root of the planet mass, that is, approximately with the linear dimensions. The horizontal error bars indicate the radial excursions that result from the planetary eccentricity. We see that Earth and Venus analogs form naturally around the location of the annulus, while Mercury and Mars analogs are often produced by remnant bodies that are scattered out of the forming region and eventually become dynamically decoupled.

ガス惑星（木星・土星）の形成

- 原始惑星大気
  - 重力 ⇔ 微惑星落下による熱(圧力）　で平衡
    - Kelvin-Helmholz time (cooling時間)

$$t_{\mathrm{KH}} \approx GM_{\mathrm{core}}M_{\mathrm{atm}}/RL \approx 10^{10}(M_{\mathrm{core}}/M_{\oplus})^{-3.5}\mathrm{yr}$$

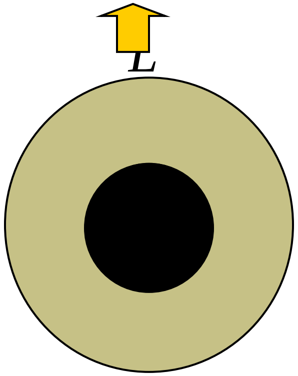

Ikoma et al. (2000)

比較：円盤ガスの存在時間

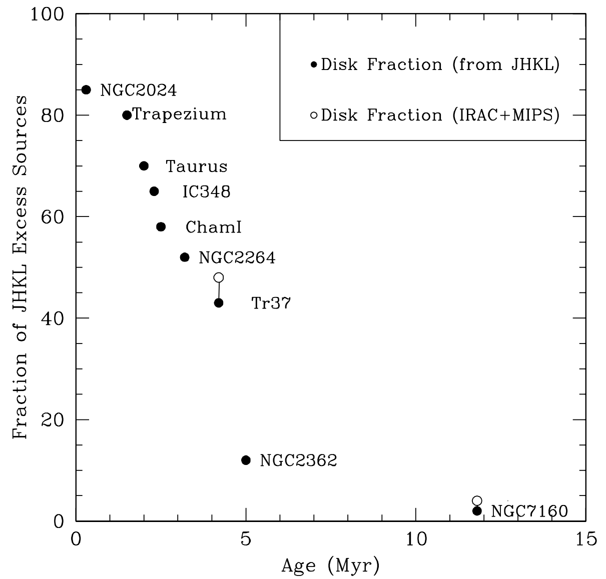

Fig. 13.—Evolution of the disk fraction (based on *JHKL* excesses) vs. age. We display the disk fraction data compiled by Haisch et al. (2001), based on the detection of *JHKL* excesses, with the disk fractions estimates in Tr 37 and NGC 7160, using the *JHK* and 3.6 μm excesses. We also display disk fractions estimated from excesses in the longer wavelength IRAC bands and/or the MIPS 24 μm flux (*open circles*). The Cep OB2 data are consistent with the dissipation of disks in ~10 Myr.

Sicilia-Aguilar et al. 2006a

惑星へのガス降着

Tanigawa et al. 2012

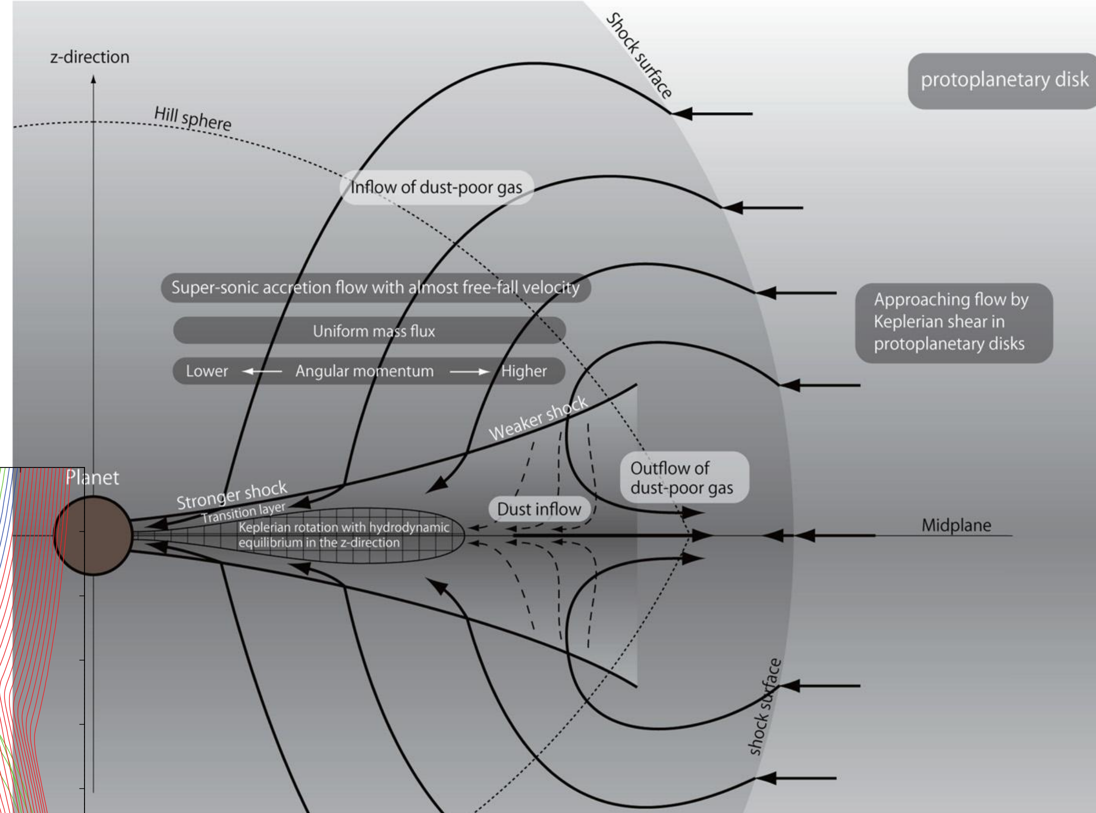

Figure 17. Schematic picture of the flow structure of circumplanetary disks.

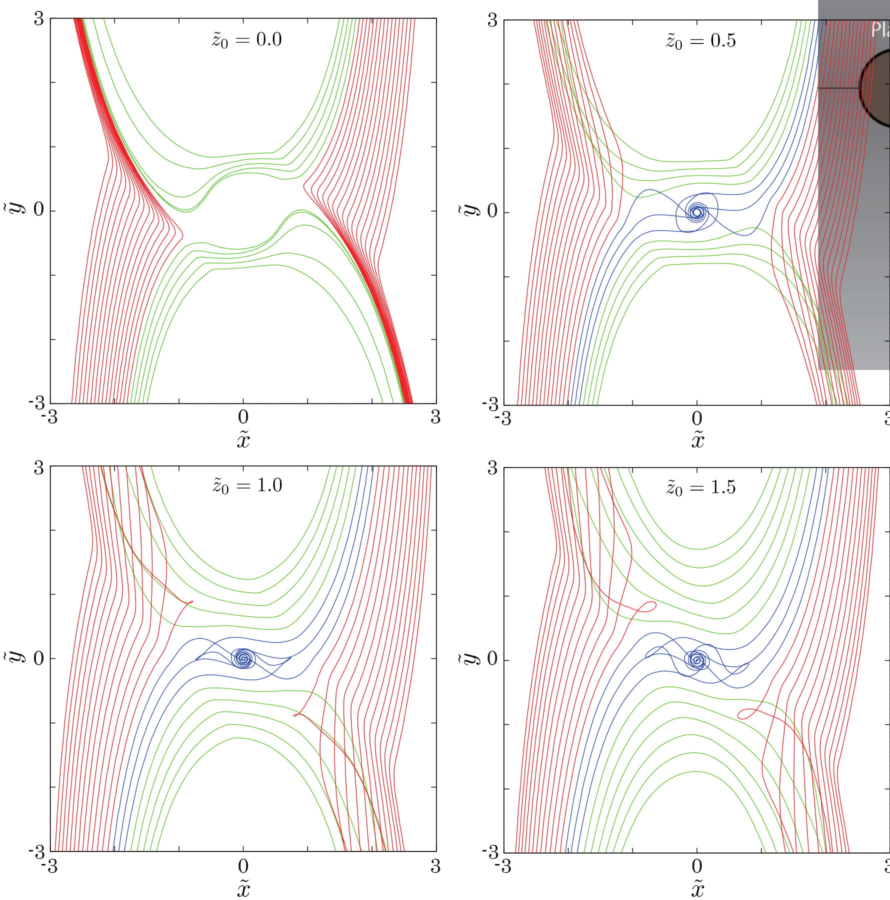

tarting from four different heights ($\tilde{z}_0 = 0.0, 0.5, 1.0, 1.5$), with $\tilde{x}_0 = [\pm 2, \pm 3]$ and $\tilde{y}_0 = \pm \tilde{L}_y/2$. The interval of the starting points is 0.05 in
blue, and red curves show streamlines in the horseshoe, accretion, and passing regions, respectively.

周惑星円盤：

- 惑星への質量供給
- 衛星形成

参考文献

- Hansen, B., 2009. FORMATION OF TERRESTRIAL PLANETS FROM A NARROW ANNULUS, The Astrophysical Journal 703, 1131-1140.
- Hasegawa, M., et al 1988. Gravitational Scattering between Planetesimals and Their Statistical Behavior, Progress of Theoretical Physics Supplement No.96 175-195
- Kokubo, E., and S. Ida 1998.Oligarchic Growth of Protoplanets, Icarus 131, 171–178
- Kokubo, E., and S. Ida 2000. Formation of Protoplanets from Planetesimals in the Solar Nebula, Icarus 143, 15–27
- Kokubo, E., and S. Ida 2002. FORMATION OF PROTOPLANET SYSTEM AND DIVERSITY OF PLANETARY SYSTEMS, The Astrophysical Journal 581, 666–680
- Nishida, S. 1983. Collisional Processes of Planetesimals with a Protoplanet under the Gravity of the Proto-Sun, Progress of Theoretical Physics Vol.70 93-105
- Sicilia-Aguilar, A, et al., 2006. Disk Evolution in Cep OB2: Results from the Spitzer Space Telescope, The Astrophysical Journal, Vol 638, 897-919
- Tanigawa, T, K, Ohtsuki, and M, Machida., 2012. Distribution of Accreting Gas and Angular Momentum onto Circumplanetary Disks, The Astrophysical Journal, Vol 747, 47